Pharm Res (2014) 31:2887–2903
DOI 10.1007/s11095-014-1385-4

RESEARCH PAPER

Enhancement of the Physical Stability of Amorphous Indomethacin by Mixing it with Octaacetylmaltose. Inter and Intra Molecular Studies

E. Kaminska • K. Adrjanowicz • D. Zakowiecki • B. Milanowski • M. Tarnacka • L. Hawelek • M. Dulski • J. Pilch • W. Smolka • I. Kaczmarczyk-Sedlak • K. Kaminski

Received: 10 January 2014 / Accepted: 7 April 2014 / Published online: 15 May 2014

ABSTRACT

Purpose To demonstrate a very effective and easy way of stabilization of amorphous indomethacin (IMC) by preparing binary mixtures with octaacetylmaltose (acMAL). In order to understand the origin of increased stability of amorphous system inter- and intramolecular interactions between IMC and acMAL were studied.

Methods The amorphous IMC, acMAL and binary mixtures (IMC–acMAL) with different weight ratios were analyzed by using Dielectric Spectroscopy (DS), Differential Scanning Calorimetry (DSC), Raman Spectroscopy, X-ray Diffraction (XRD), Infrared Spectroscopy (FTIR) and Quantitative Structure–Activity Relationship (QSAR).

Results Our studies have revealed that indomethacin mixed with acetylated saccharide forms homogeneous mixture. Interestingly, even a small amount of modified maltose prevents from recrystallization of amorphous indomethacin. FTIR measurements and QSAR calculations have shown that octaacetylmaltose significantly affects the concentration of indomethacin dimers. Moreover, with increasing the amount of acMAL in the amorphous solid dispersion molecular interactions between matrix and API become more dominant than IMC-IMC ones. Structural investigations with the use of X-ray diffraction technique have demonstrated that binary mixture of indomethacin with acMAL does not recrystallize upon storage at room temperature for more than 1.5 year. Finally, it was shown that acMAL can be used to improve solubility of IMC.

Conclusions Acetylated derivative of maltose might be very effective agent to improve physical stability of amorphous indomethacin as well as to enhance its solubility. Intermolecular interactions between modified carbohydrate and IMC are likely to be responsible for increased stability effect in the glassy state.

KEY WORDS crystallization · glass transition · indomethacin · intermolecular interactions · molecular dynamics · octaacetylmaltose · physical stability

INTRODUCTION

Indomethacin (IMC) is non-steroidal anti-inflammatory drug (NSAID), being also known as a model amorphous pharmaceutical substance. It is widely used to treat pain, fever,

E. Kaminska (✉) • I. Kaczmarczyk-Sedlak
Medical University of Silesia in Katowice, School of Pharmacy with the Division of Laboratory Medicine in Sosnowiec, Department of Pharmacognosy and Phytochemistry, ul. Jagiellonska 4, 41-200 Sosnowiec, Poland
e-mail: ekaminska@sum.edu.pl

K. Adrjanowicz
NanoBioMedical Centre, Adam Mickiewicz University ul. Umultowska 85 61-614 Poznan, Poland

D. Zakowiecki
Pharmaceutical Works Polpharma SA ul. Pelplinska 19, 83-200 Starogard Gdanski, Poland

B. Milanowski
Department of Pharmaceutical Technology, Poznan University of Medical Sciences, ul. Grunwaldzka 6 60-780 Poznan, Poland

M. Tarnacka • L. Hawelek • M. Dulski • K. Kaminski
Institute of Physics, Silesian University ul. Uniwersytecka 4 40-007 Katowice, Poland

L. Hawelek
Institute of Non-ferrous Metals ul. Sowinskiego 5, 44-100 Gliwice, Poland

J. Pilch
Department of Biological Sciences, Academy of Physical Education ul. Raciborska 1, 40-074 Katowice, Poland

W. Smolka
Department of Laryngology, Medical University of Silesia ul. Francuska 20-24, 40-027 Katowice, Poland

stiffness, swelling and inflammation caused by many conditions such as arthritis, gout, ankylosing spondylitis, bursitis or tendinitis (www.drugbank.ca) (1,2). It may also be used for other purposes: in cardiovascular (3) and Alzheimer diseases (4), cancer prevention (5) etc. IMC inhibits the cyclooxygenase (COX) – 1 and 2 enzyme, necessary for the formation of prostaglandins (hormone-like molecules normally found in the body) and other autacoids (6–8). Indomethacin in the crystalline form is practically insoluble in water (experimental solubility was determined to be 0.937 mg/L at 298 K (www.drugbank.ca)). It belongs to the second class of Biopharmaceutical Classification System (BCS) (9,10), i.e. drugs characterized by low solubility and high permeability (11).

To increase the solubility of indomethacin and other poorly water-soluble drugs (of the 2nd and 4th class of BCS system) diverse approaches can be employed (11–25). Some of them are: i) the use of pro-drugs, ii) salt formation (tatrate, succinate, mesylate, nitrate, hydrochloric), iii) micronization, iv) cocrystallization (23), v) solid dispersions with soluble polymers, saccharides and vi) amorphization. As demonstrated in numerous reports converting crystalline substance into amorphous one seems to be the most promising method (16,17,19,24,25). In order to induce such conversion some routine physical processing including melt quenching (13,15,16), freeze- (26) and spray-drying (26–28), milling or cryomilling (29), pressurization of crystals (30), compression of liquid (31) and vapor deposition (32–34) can be applied. However, the simplest method is quench cooling of a molten crystal (called commonly vitrification). Unlike their crystalline counterparts, amorphous materials dissolve faster and have greater solubility due to higher free energy and specific volume of the amorphous state (16,17,19,24,25,35–37). Solubility of amorphous IMC is approximately four times greater than that of the most stable γ-polymorphic form (17,36). Moreover, the chemical reactivity (13,38) as well as compressibility abilities (15,39) of amorphous active ingredients can be also significantly enhanced, when compared to the crystalline counterparts. Unfortunately, due to thermodynamic properties amorphous APIs are prone to recrystallization during processing, storage and use of the product (25,40). Consequently, the advantages given in terms of better solubility and bioavailability can be completely lost. Additionally, amorphous pharmaceuticals may undergo chemical degradation as well as isomeric transformations during manufacturing (41,42). Therefore, it is very important to understand the role of the most important factors responsible for physical as well as chemical instability of these materials. This seems to be the crucial point in the course of developing effective ways of stabilizing amorphous APIs.

As it is believed, the tendency towards recrystallization from the amorphous state depends on the molecular mobility that is very slow at temperatures well below the glass-transition temperature, T_g. Under these conditions, configurational entropy seems to be frozen so the molecular mobility reduces to the local reorientation, mostly noncooperative motions of some parts of molecules that may trigger crystallization process. For most amorphous pharmaceuticals, storage at temperature ~50 K below T_g is thought to be safe due to the time scale of structural relaxation that exceeds typical shelf-life of pharmaceutical product (43). However, as shown in the case of indomethacin, recrystallization can be observed even 100 K below the glass transition temperature (25,40,43,44). Since local molecular mobility was proposed to be responsible for the recrystallization of IMC molecular dynamics in the glassy state was studied by several experimental techniques such as differential scanning calorimetry (DSC) (45–47), thermomechanical analysis (48), dielectric spectroscopy (DS) (31,49–51), isothermal microcalorimetry TAM (52), thermally stimulated depolarized current (TSDC) (53,54) and nuclear magnetic resonance (NMR) (51,55). However, despite of application of so many sophisticated methods the link between local mobility and crystallization ability of amorphous IMC remains still very controversial issue and has not been clarified yet.

Most of recent studies explore new ways to obtain stable amorphous form of this API (33,34,37,56–59). It was shown that the glassy indomethacin obtained by very slow cooling of a liquid is stable against crystallization over 2 years (25,40), while the one prepared by the fast quench cooling crystallizes more rapidly. On the other hand, amorphous IMC obtained by cryogenic grinding is the least stable and recrystallizes up to 90% after approximately 13–15 h (56,60). Ediger's group has shown that highly stable indomethacin glass prepared by vapour deposition (32–34,61) has lower enthalpy (8 J/g) and greater density compared to the ordinarily obtained glass. It should be also stressed that preparation of homogeneous solid dispersion consisted of IMC and excipient, typically saccharide or polymer turned out to be one of the best method to improve physical stability as well as solubility of this active pharmaceutical ingredient (18,62–72).

Recently Grzybowska *et al.* have shown that carbohydrate derivative, different from the ones used so far by others, can be good stabilizer of amorphous API (73,74). As it turned out, extended physical stability of the amorphous binary system of celecoxib with only 10 wt% octaacetylmaltose was achieved (no signs of the sample recrystallization after 9 months of storage at room temperature). This is very promising result taking into account that amorphous celecoxib is very unstable and recrystallizes almost completely (90%) just after 10 days of storage at similar conditions. Simultaneously, solubility of amorphous binary mixture CEL-acMAL in water was more than ten folds greater than crystalline pharmaceutical (74). Based on molecular dynamics studies it was concluded that reduced crystallization ability of celecoxib comes from the significant slowing down of the local mobility in the glassy state. Moreover DFT calculations and computer simulations showed that celecoxib and octaacetylmaltose form very effective hydrogen bonds that prevent from recrystallization of amorphous API.

Very recently another application of acetyl saccharides has been reported. In paper (75) some of us showed that acetylated saccharides can protect labile diuretic API, furosemide, against physical as well as chemical instability. Moreover, the solubility of the analyzed furosemide - modified saccharide mixtures, was significantly enhanced with respect to the crystalline form of this active ingredient.

In this paper we have demonstrated, that acetylated derivative of maltose (octaacetylmaltose) might be very effective in stabilizing amorphous form of indomethacin. Our detailed molecular dynamics studies have indicated that IMC in acMAL matrix doesn't tend to recrystallize even when heated much above the glass transition temperature. We have also demonstrated that solid dispersion of IMC with octaacetylmaltose is homogeneous and no phase separation occurs in the whole studied range of temperatures. Moreover, solubility of IMC-acMAL binary mixtures turned out to be greater than that of the pure crystalline IMC. Finally, FTIR measurements and QSAR calculations revealed strong interactions between API and acMAL which might be responsible for long term stability of amorphous IMC in the solid dispersion.

EXPERIMENTAL METHODS

Materials

The γ-crystalline form of Indomethacin (1-(4-Chlorobenzoyl)-5-methoxy-2-methyl-3-indoleacetic acid, $C_{19}H_{16}ClNO_4$, Mw = 357.8 g/mol) was generously provided by GlaxoSmithKline Pharmaceuticals S.A. (Poznan, Poland) as a gift sample. The purity of a drug was declared by supplier as 99.6%. Octaacetylmaltose ($C_{28}H_{38}O_{19}$, Mw = 678.6 g/mol), having purity greater than 98%, was purchased from Sigma-Aldrich Co. LLC (Poznan, Poland). Materials were used without further purification. The chemical structures of both compounds are shown in Scheme 1.

One can add that each measurement presented in this paper was repeated at least once. In the case of solubility studies three experiments were performed.

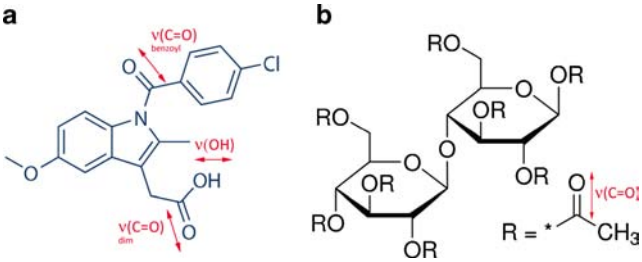

Scheme 1 The chemical structure of indomethacin (**a**) and octaacetylmaltose (**b**). In addition vibrations of hydroxyl and carbonyl groups used in infrared analysis were denoted.

METHODS

Preparation of Amorphous Systems of Indomethacin with Octaacetylmaltose by Quench Cooling

The amorphous IMC, acMAL and binary systems IMC-acMAL with different weight ratios of acMAL were prepared by the quench cooling technique in the temperature and humidity controlled glovebox (PLAS LABORATORIES Inc. 890-THC-DT/EXP/SP) at the assured relative humidity RH < 10%. In order to obtain the homogeneous IMC-acMAL mixtures, first we thoroughly mixed crystalline powders of both compounds in appropriate proportions in a heat-resistant glass vial (weight of powder mixture was about 0.5 g). After that we put the magnetic stir bar into the vial with the mixture. Next, the crystalline components was melted in the vial on the hot plate magnetic stirrer (CAT M 17.5) at T = 443.15 K. The temperature inside the vial was controlled by using Pt-100 sensor. After the crystalline mixture IMC-acMAL was fully melted it was transferred from the hot plate to a very cold metal plate. The amorphous samples obtained in this way were analyzed immediately after the preparation. We investigated three mixtures of indomethacin and octaacetylmaltose with different weight fraction of IMC (Table I). However, one should mention, that FTIR, Raman and solubility measurements were also carried out for additional solid dispersions with lower and higher content of IMC.

Differential Scanning Calorimetry (DSC)

Thermodynamic properties of amorphous forms of indomethacin, octaacetylmaltose and their mixtures (1 : 1, 1 : 3, and 3 : 1 weight ratios) have been investigated by differential scanning calorimetry. Calorimetric measurements were carried out using double-furnace, power-compensation DSC 8000 PerkinElmer apparatus equipped with a liquid nitrogen cooling accessories and platinum resistance thermometers. Temperature and enthalpy calibrations were performed with indium standard. Amorphous samples and their binary mixtures were scanned at a rate of 10 K/min over a temperature range of 220 K to well above the respective melting points.

Table I The Investigated Mixtures of Indomethacin (IMC) with Octaacetylmaltose (acMAL)

System	IMC pure 100%	75% w/w IMC in acMAL	50% w/w IMC in acMAL	25% w/w IMC in acMAL	acMAL 100%
Weight ratio (m_{IMC} : m_{acMAL})	1 : 0	3 : 1	1 : 1	1 : 3	0 : 1
Weight fraction of indomethacin (X_{IMC})	1	0.75	0.5	0.25	0

Broadband Dielectric Spectroscopy (DS)

Isobaric dielectric measurements were carried out using a Novo-Control Alpha dielectric spectrometer (Novocontrol Technologies GmbH & Co. KG, Hundsangen, Germany). Our experiments covered frequency range from 10^{-2} to 3×10^{6} Hz and temperature range from 133 to 364 K. The temperature was controlled using a nitrogen-gas cryostat with temperature stability better than 0.1 K. Samples were placed in a parallel plate cell (diameter: 20 mm, gap: 0.1 mm). The capacitor was made from a stainless steel. Dielectric measurements of IMC, modified carbohydrate as well as solid dispersions were performed after their vitrification by fast cooling from the melting point.

Raman Spectroscopy

Confocal Raman microscopy was performed using WITec alpha300 R system equipped with Nd:YAG laser (532 nm at 40 mW of power) and a high sensitivity back-illuminated Newton-CCD camera captured the spectra. A 200 μm× 200 μm area using 200×200 pixels (=40 000 spectra) with an integration time of 50 ms per spectrum was analyzed. The data were collected at a 50X Olympus objective with a 0.76 numerical aperture, at a nominal resolution of 2 cm^{-1} and a precision of ±1 cm^{-1} in the range between 120 and 4,000 cm^{-1}. The temperature Raman measurements were also carried out with accuracy of ±5 K/min.

X-ray Diffraction (XRD)

The long-term isothermal X-ray diffraction measurements for the crystalline IMC, crystalline acMAL and amorphous mixtures of IMC with acMAL were carried out at room temperature (T=293 K) on the laboratory Rigaku-Denki D/MAX RAPID II-R diffractometer attached with a rotating anode Ag Kα tube (λ=0.5608 Å), an incident beam (002) graphite monochromator and an image plate in the Debye–Scherrer geometry. The pixel size was 100 μm×100 μm. The samples were placed inside Lindemann glass capillaries (1.5 mm in diameter). Measurements were run with the sample filled and empty capillaries, and the intensity for the empty capillary was then subtracted. The beam width at the sample was 0.1 mm. The two-dimensional diffraction patterns were converted into the one-dimensional intensity data using suitable software provided by Rigaku Corporation.

Infrared Spectroscopy (FTIR Spectroscopy)

Infrared measurements were carried out using a Agilent Cary 660 FTIR spectrometer equipped with a standard source and a DTGS Peltier-cooled detector. The spectra have been collected using GladiATR diamond accessory (Pike Technologies) in the 4,000–400 cm^{-1} range. All spectra were accumulated with a spectral resolution of 4 cm^{-1} and recorded by accumulating of 16 scans.

Quantitative Structure–Activity Relationship (QSAR) Calculations

The geometry of IMC-acMAL binary system was optimized using the B3LYP exchange-correlation functional (76–78) and 6-31G(d,p) basis set. The calculations were carried out in gas phase using density functional theory (DFT) (79–81) and the Gaussian 09 software package (82). The optimized structure was used as input files to calculate the wave functions by the DIRECT self-consistent field algorithm of Gaussian 09. The molecular electron densities and molecular electrostatic potential surface of IMC-acMAL binary system were determined from the wave functions using CUBE option implemented in Gaussian 09 and visualized using GaussView 5.0. A color map for potential surface was chosen to get maximum contrast for a system of a given net charge. The relative locations of partial positive and negative charge were found to be independent of the choice of basis set.

Solubility Study

The solubility study was performed by a traditional shake-flask technique. The samples were pulverised and put into conical flasks containing suitable solvent, then were shaken in a water bath at the temperature of 310 K for 2 h. Obtained solutions were filtered through Syringe Filters 0.45 μm (Pall Poland Ltd, Warsaw, Poland). The determination of the amount of dissolved API proceeded using the GENESYS 10S UV–vis spectrophotometer (Thermo Scientific, Waltham, MA, USA) at the wavelength of 266 nm in a 1 cm pathlength cell. The solubility was investigated in compendial dissolution solvents prepared in accordance to Ph. Eur. Monograph 2.9.3. representing the physiological pH range of the human gastro intestinal tract. Solvents such as 0.1 M hydrochloric acid (pH 1.2), acetate buffer solution pH 4.5, phosphate buffer solution pH 6.8 and purified water (pH≈6.9–7.0) were used.

RESULTS AND DISCUSSION

It was previously mentioned, that indomethacin prepared in the amorphous form is unstable and crystallizes when stored well below (T_g – 50 K) the glass transition temperature. This finding made IMC a model pharmaceutical to study mechanism of recrystallization from the glassy state. Recently we have proposed new type of materials that can be used to ensure stability of labile active ingredients (celecoxib and furosemide). As shown in papers (74) and (75), acetylated saccharides may be an alternative for standard excipients like PVP or inulin for several reasons: i) they are nontoxic, (ii) they

reveal no tendency toward crystallization (iii) they do not undergo thermal decomposition during the melting process (in contrast to the natural saccharides, acetylated carbohydrates do not caramelize) and finally (iv) they strongly interact with APIs.

Herein we have decided to check if octaacetylmaltose can be used to stabilize amorphous form of a model drug—indomethacin. To obtain the solid dispersion of IMC with acMAL quench cooling of the molten solution was applied. Because of the similar melting temperatures of IMC (T_m=431 K) and acMAL (T_m=432 K) uniform mixtures were prepared quickly and thoroughly without the risk of components overheating and chemical decomposition. It turned out, that indomethacin mixes very well with acetylated maltose in the studied range of weight ratios. It is worth noting that in contrast to other amorphization methods such as freeze-, spray drying, solvent evaporation (e.g., used, for example, to obtain IMC-PVP or IMC-isomalt dispersions (67,68,83)), quench cooling does not require using any additional solvent and further purification of the sample.

To study and characterize physical properties of obtained solid dispersions different experimental techniques were employed. As a first, DSC and DS methods were applied to investigate thermodynamical and dynamical properties of binary mixtures (IMC – acMAL) with different content of acMAL.

Representative DSC thermograms of studied herein systems are shown in Fig. 1a–e. As demonstrated, there is only one characteristic endothermic event associated with the glass transition phenomenon in all cases (values of T_g calculated from DSC measurements are listed in Table II). Furthermore there is no sign of cold crystallization in the studied samples. This is very interesting result in view of long term physical stability of amorphous IMC dispersed in the carbohydrate matrix. Since beside of the one endothermic event associated to the glass transition there are no others heat capacity jumps in thermograms presented in Fig. 1. One could claim that our sample are homogeneous in the range of studied temperatures. However, it should be noted that even in the phase separating multicomponent heterogeneous systems one glass transition can be observed. Thus, further dielectric as well as optical measurements were carried out to verify whether investigated samples were homogeneous indeed.

In Fig. 2. dielectric loss spectra of indomethacin (b), octaacetylmaltose (a) and their representative mixtures in a 1 : 1 (c) and 1 : 3 (d) weight ratios, obtained at several temperatures below and above T_g are presented. As demonstrated, two characteristic features can be identified in loss spectra. The first one, reflected as a straight line with the slope log $\omega \approx f^{-1}$, is a dc conductivity that is connected to the charge transport within the sample. The second one is a loss peak called structural (α) relaxation process. It is related to the viscous flow and the glass transition event. With lowering temperature both processes move towards lower frequencies. Below T_g relaxation time of the structural process becomes too long to be observed in the experimental frequency window. In the glassy state one well separated secondary process (we labelled it as a γ) can be observed for both pure IMC and acMAL as well as for the solid dispersions. For indomethacin, the molecular origin of the γ-process has been previously discussed in literature (31,51). Detailed studies with the use of dielectric and NMR spectroscopies suggested chlorobenzyl groups' rotation (51) to be responsible for this process detected in dielectric loss spectra. Interestingly Carpenter *et al.* hypothesized that there is also another relaxation mode (β) that is hidden under high frequency part of the structural process

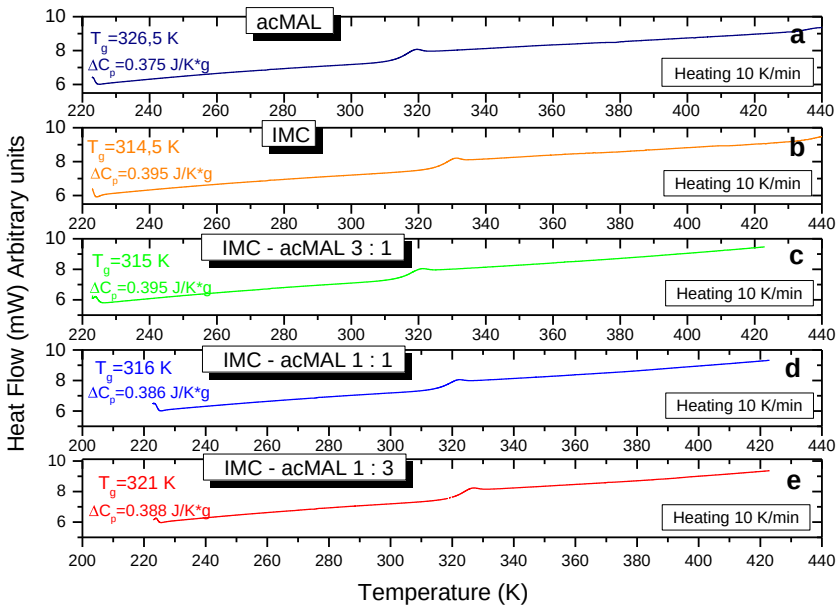

Fig. 1 DSC curves of acMAL – *navy line* (**a**), IMC – *orange line* (**b**), mixtures of IMC and acMAL 3: 1 weight ratio (**c**) – *green line*, mixtures of IMC and acMAL 1: 1 weight ratio – *blue line* (**d**), mixtures of IMC and acMAL 1: 3 weight ratio – *red line* (**e**). The samples have been heated at 10 K/min from T = 220 K to T = 440 K.

Table II Glass Transition Temperatures (T_g's) and Isobaric Fragilities (m_p) for Investigated Systems Obtained from Dielectric Measurements. Values of the Glass Transition Temperatures T_g's and Heat Capacity Jumps at T_g (Δc_p) Determined from DSC Curves are Also Shown

[a] m_p i T_g were calculated for $\tau_\alpha = 100$ s

Material	T_g [K] from DSC measurements	T_g [K][a] from dielectric measurements	Fragility m_p[a] from dielectric measurements	Δc_p [J/K*g] from DSC measurements
Indomethacin (IMC)	314.5	315	86	0.395
Octaacetylmaltose (acMAL)	326.5	329	106	0.375
IMC : acMAL (3 : 1)	315	311	77	0.395
IMC : acMAL (1 : 1)	316	311	81	0.386
IMC : acMAL (1 : 3)	321	317	84	0.388

(51). In fact high pressure measurements (31) confirmed this thesis. On the other hand experimental investigations supported by theoretical calculations showed that γ-process in modified maltose originates from the motions of the acetyl moieties attached to the saccharide ring (74,75,84). What is more it was found that due to the steric hindrance (acetyl groups) the structure of octaacetylmaltose seems to be very rigid. One can add that twisting motions around the glycosidic linkage are significantly suppressed in such material. Consequently modified carbohydrate becomes an ideal stabilizer for labile APIs (84).

As seen in Fig. 2, there is also one secondary process (denoted as a γ-relaxation) observed in dielectric loss spectra of solid dispersions. It is supposed that in these cases observed relaxation process is connected to the intramolecular motions within IMC and modified carbohydrate. However, due to the resolution of our set up contribution of secondary relaxation processes of single components can't be resolved. Herein, it is worth to remind that an addition of a second compound may be very useful to separate and visualize the slow β-relaxation process from the excess wing of the first component (85–90). For example, such scenario was observed by Blochowicz and

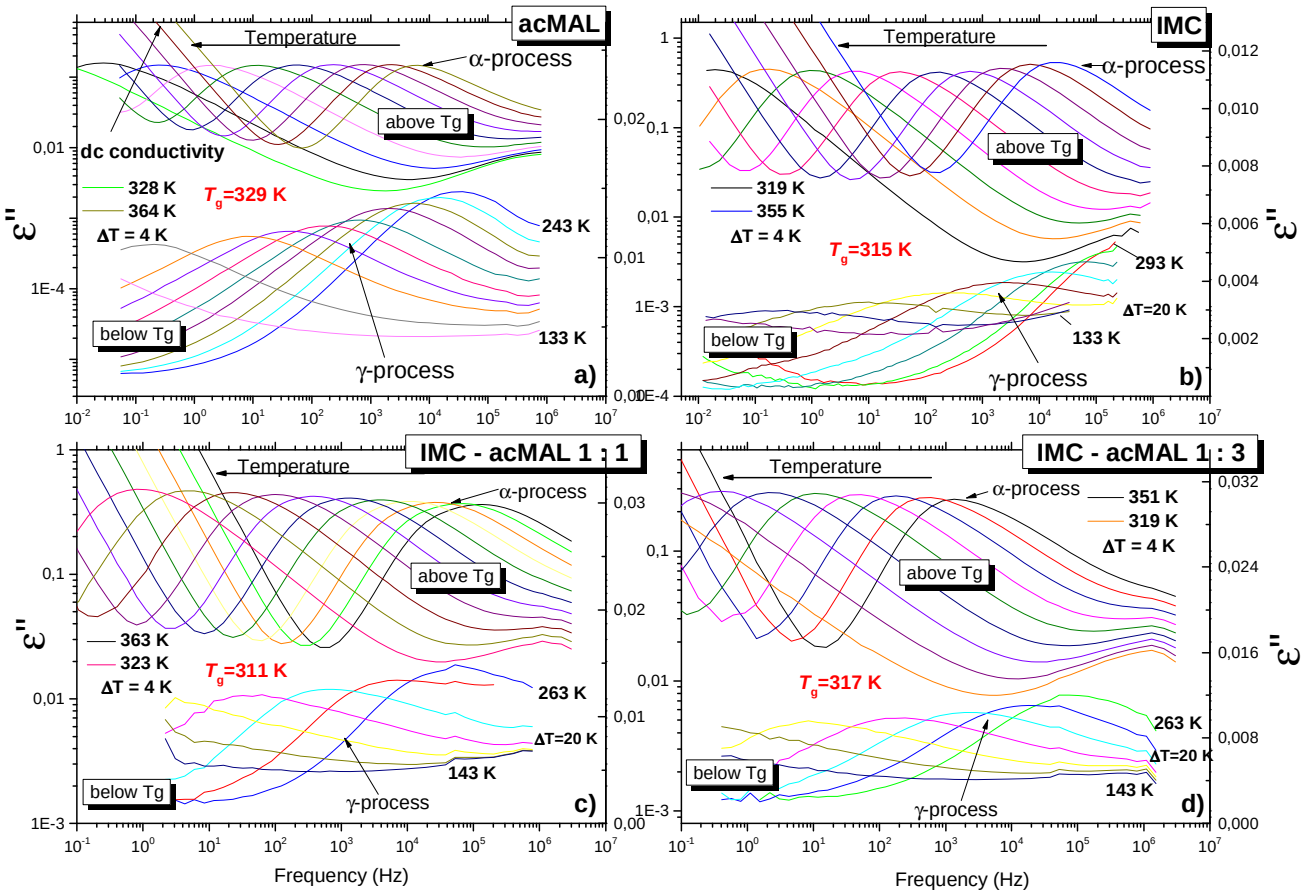

Fig. 2 Frequency-dependent dielectric loss spectra for pure acMAL (**a**), IMC (**b**), and representative binary mixtures: IMC - acMAL 1 : 1 weight ratio (**c**), IMC - acMAL 1 : 3 weight ratio (**d**) measured at ambient pressure ($P = 0.1$ MPa) and different temperatures above and below T_g.

Rössler in 2-picoline mixed with various oligostyrenes (85). However, slow β-process of IMC has not been detected in the case of studied herein dispersions.

One should also add that obtained dielectric data were used to certify homogeneity of the samples. As it is shown in Fig. 2 there is only one structural relaxation process above T_g. In this context it is worth to mention the paper by Power *et al.* (91) where two relaxation processes coming from the single components in the microphase separating systems were detected in dielectric spectra. Moreover, it was also demonstrated that another relaxation process called usually Maxwell - Wagner appears in loss spectra of heterogeneous samples such as colloids, suspensions, phase separating binary mixtures, polymer blends etc. (92). It is related to an additional interfacial polarization that is induced in these systems. After closer inspection of measured loss as well as dispersion spectra (data not shown) one can rule out such scenario and conclude that investigated herein samples were homogeneous.

In Fig. 3 representative dielectric loss spectra of pure IMC, acMAL and their representative mixtures (3 : 1 and 1 : 1 weight ratios) measured at selected temperatures close to T_g are compared. As illustrated, the shape of the structural peak for acMAL and mixtures are nearly the same, whereas the α-peak of IMC is slightly narrower. By fitting the alpha peaks to the one-sided Fourier transform of the Kohlrausch-Williams-Watts (KWW) function (93,94)

$$\varepsilon'' = \Delta\varepsilon \int_0^\infty dt \left[-\frac{d}{dt} \exp\left(-\frac{t}{\tau_k} \right)^{\beta_{KWW}} \right] \sin(2\pi f t) \qquad (1)$$

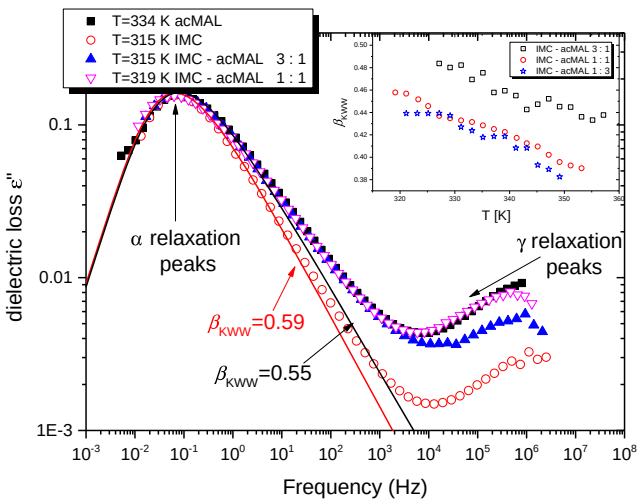

Fig. 3 Comparison of representative dielectric loss spectra measured at indicated temperatures near T_g for pure IMC, pure acMAL and 3 : 1 and 1 : 1 IMC - acMAL mixtures. *Solid lines* represent KWW fits with the stretching exponent equal to β_{KWW} = 0.59 (IMC) and 0.55 (acMAL, mixtures of IMC with acMAL). In the *inset* the temperature dependences of β_{KWW} for the investigated solid dispersions are presented.

the same value of the stretching parameter β_{KWW} = 0.55 for acMAL and both mixtures of IMC- acMAL was obtained. In the case of IMC β_{KWW} is equal to 0.59. The similar results for pure components, IMC and acMAL were reported earlier (31,51,74,84).

It is worth noting, that in the case of solid dispersions an additional analysis of the temperature dependencies of the β_{KWW} parameter was carried out to make further verification of homogeneity of the investigated systems. In the inset to Fig. 3 a stretching parameter β_{KWW} is plotted *versus* temperature. It should be noted that β_{KWW} was calculated from the Havriliak- Negami parameters using the following formula (95):

$$\alpha^*\beta = \beta_{KWW}{}^{1.23} \qquad (2)$$

where α and β are parameters describing slopes of the high and low frequency part of the structural relaxation process (it is important to emphasize, that β_{KWW} estimated from Eqs. 1 and 2 can be different). As demonstrated, β_{KWW} changes within the experimental uncertainty indicating that the shape of the structural relaxation process is temperature independent. In this context it is worth to recall again to paper by Power *et al.* (91), where the behaviour of α-relaxation process in the mixtures of 5-methyl-2-hexanol and isoamylbromide was analysed. The authors have shown that in such system nanoseparation might occur, as indicated by the significant variations of the static permittivity and the shape of the structural relaxation process with temperature. It should be also noted that Power *et al.* investigated mixtures consisted of liquids that differ in viscosities, densities and glass transition temperatures. On the other hand, octaacetylmaltose and indomethacin have similar melting temperatures, densities (ρ = 1.37 g/cm^3 (http://www.chem-info.com)—acMAL and ρ = 1.38 g/cm^3 – IMC (51,96)), viscosities and T_gs. Hence, the observed features including: i) one structural relaxation process of almost invariant shape, ii) the absence of any unexpected variation of the static permittivity (data not shown) and Maxwell - Wagner relaxation are clear indications that solid dispersions formed by IMC and acMAL are homogeneous indeed.

In order to reconfirm homogeneity of prepared solid dispersions Raman Spectroscopy was applied. Confocal Raman Microscopy (CRM) allows to investigate the spatial distribution of chemical compounds in the entire volume of the sample. The spectral resolution of the CRM is more than sufficient (below 1 μm) to check the homogeneity of the mixture. The Raman spectra of IMC-acMAL systems as well as Raman integral intensity analysis for some characteristic bands associated with IMC and acMAL were performed. Results of our measurements are presented in Fig. 4. Accordingly to the infrared analysis given by Strachan *et al.* (97) we have selected four

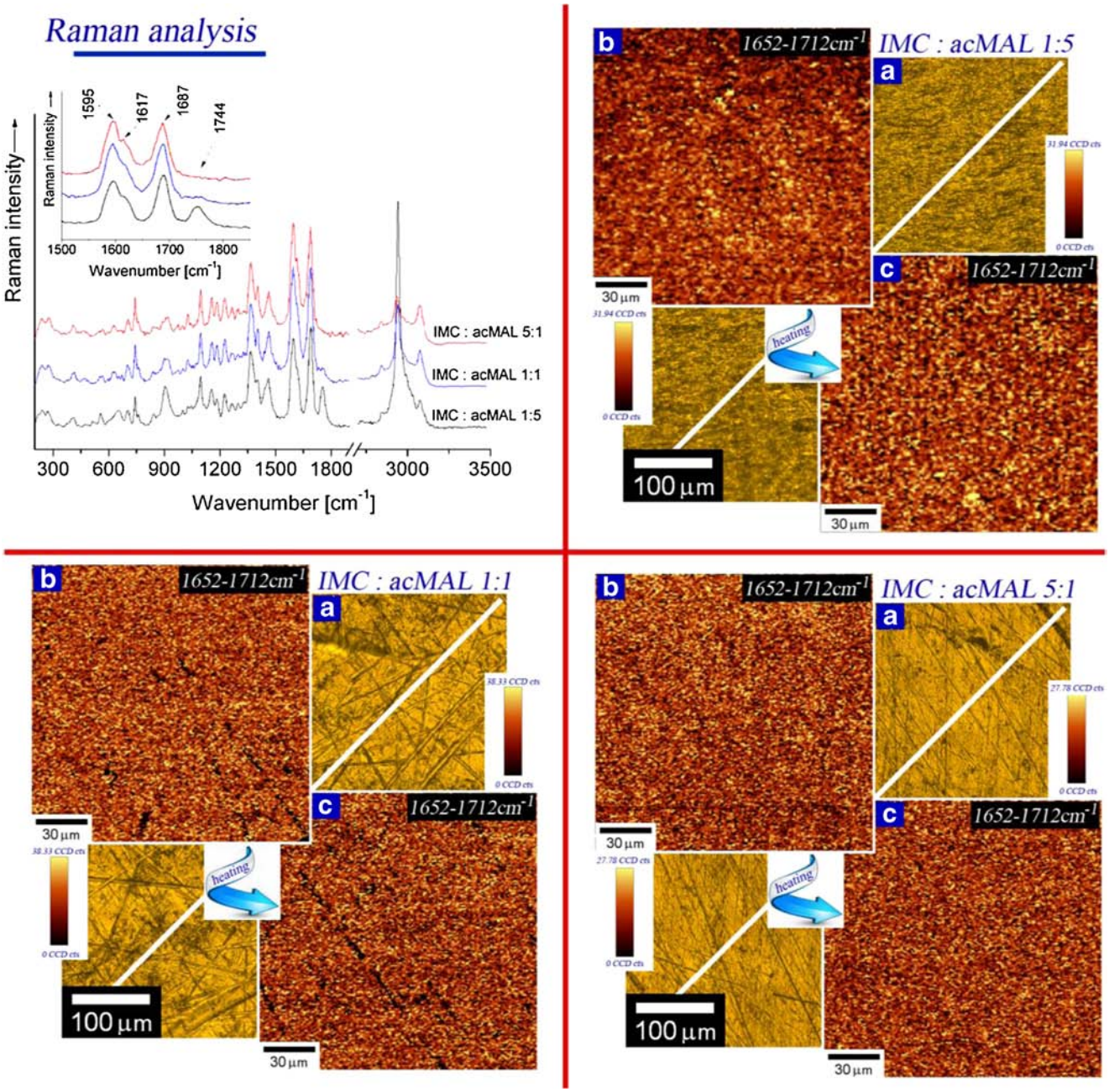

Fig. 4 The Raman spectra of IMC - acMAL binary systems (5 : 1, 1 : 1, 1 : 5 weight ratios), (**a**) optical map and integral intensity Raman analysis for band in the 1,652–1,712 cm^{-1} range at (**b**) 298 K, (**c**) 343 K.

characteristic bands for indomethacin and acetyl derivative of maltose. Three of them, located at 1,595, 1,617, 1,687 cm^{-1}, are associated with deformational vibrations of chlorobenzyl and indole ring as well as stretching vibration of benzoyl group, respectively. It is worth noting that these bands are shifted towards higher wavenumbers (~5 cm^{-1}) with respect to the ones previously reported in reference (97). This can be explained as due to intermolecular interactions between IMC and acMAL. Additionally, the band at 1,744 cm^{-1} originates from the stretching vibration of vC=O group in octaacetylmaltose molecules. Representative integral intensity analysis for band associated with benzoyl group for each IMC-acMAL solid dispersion was carried out to verify their homogeneity. The Raman maps measured at T=298 K and T=343 K showed homogeneous distribution of integral intensity in the region of 1,652–1,712 cm^{-1}. One can add that similar results were also observed for the other bands. This is clear evidence that our solid dispersions are uniform mixtures in the entire volume (see Fig. 4). It should be also noted that investigated samples remain homogeneous in very broad range of temperatures located far above as well as below the room temperature.

In order to characterize molecular dynamics of our homogeneous binary mixtures dielectric spectra were analysed with the use of Havriliak-Negami function (98). Then, structural as well as secondary relaxation times were plotted *versus* inverse of temperature, as illustrated in Fig. 5. Temperature dependences of structural relaxation times were described by using Vogel-Fulcher-Tamman-Hesse (VFTH) equation (red lines) (99–101):

$$\tau = \tau_0 \exp\left(\frac{D_T T_0}{T - T_0}\right) \tag{3}$$

where D_T is a measure of the fragility of the analyzed relaxation process, τ_0 is a pre-exponential factor and T_0 is a VFTH temperature.

On the other hand, secondary γ-relaxation processes were fitted to the Arrhenius equation (the black solid lines):

$$\tau = \tau_0 \exp\left(\frac{E_a}{k_B T}\right) \tag{4}$$

where E_a is an activation energy barrier and k_B is a Boltzmann constant.

From the VFTH fits the glass transition temperatures for IMC (T_g=315 K), acMAL (T_g=329 K), and their 3 : 1, 1 : 1 and 1 : 3 solid dispersions (311 K, 311 K, 317 K, respectively) were determined. Herein, the glass transition temperature, T_g, was defined as a temperature at which α-relaxation time reaches 100 s. One can add, that the values of T_g for pure IMC and acMAL agree with the literature data (31,51,74,75,84). What is more, there is good agreement between T_g determined from dielectric and DSC measurements (see Table II).

Furthermore, from the Arrhenius fit (black solid lines) the values of the activation energies for the γ- relaxation processes

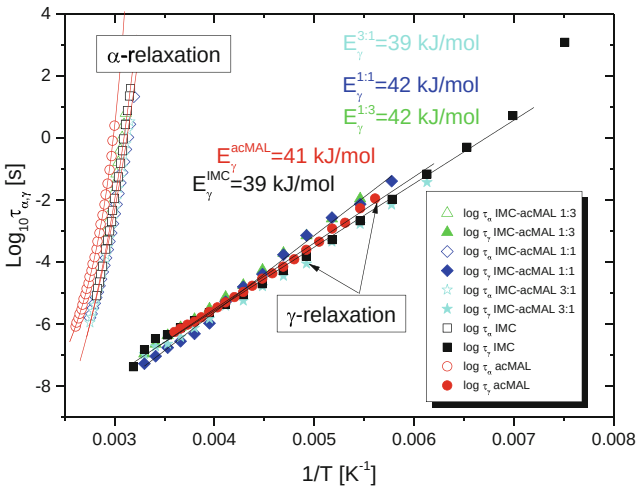

Fig. 5 Temperature dependences of the structural α - (*open symbols*), and secondary γ-relaxation times (*filled symbols*) for pure indomethacin (IMC), octaacetylmaltose (acMAL) and binary mixtures of IMC with acMAL. *Black solid lines* are fits to the secondary γ-relaxations using the Arrhenius law. The red lines represent the VFTH behaviour.

were determined. Interestingly, the activation barrier of the gamma relaxation in pure components as well as in their mixtures lies within the range E_a=39–42 kJ/mol. However, such observation is highly expected since secondary relaxation processes detected in pure IMC and acMAL are connected to the intramolecular motions of some small parts of molecules. Consequently, dynamics of these processes should not be affected by the addition of the second component.

In Fig. 6(a) and (b) the glass transition temperatures obtained from dielectric and DSC measurements were plotted as a function of weight fraction of IMC in the mixture. Both experimentally determined dependences of T_g *versus* X_{IMC} were described using the Gordon-Taylor equation (102):

$$T_g\left(X_{IMC}\right) = \frac{X_{IMC} T_{g(IMC)} + k\left(1 - X_{IMC}\right) T_{g(acMAL)}}{X_{IMC} + k\left(1 - X_{IMC}\right)} \tag{5}$$

where $T_{g\ (IMC)}$ and $T_{g(acMAL)}$ are the glass transition temperatures of pure indomethacin and pure acMAL, respectively. X_{IMC} denotes indomethacin weight fraction in the mixture. The constant k represents unequal contributions of components to the mixture and is a fitting parameter characterizing the curvature of the T_g evolution.

As illustrated in Fig. 6(b) the dependence of T_g (DSC) vs X_{IMC} is well described by the Gordon-Taylor relation with the parameter k equal to 0.32, while in the case of dielectric data k=0.1 is obtained (Fig. 6a). Hence, there is a disagreement between k estimated from two different techniques. One can add that it is due to an artificial assumption that T_g is a temperature at which dielectric structural relaxation time reaches 100 s. On the other hand there are many examples showing that T_g estimated from DSC or other experimental methods corresponds to the temperature at which τ_α=1 s, 10 s or even 1,000 s. Thus, although T_gs determined from DSC and dielectric data seem to be very close, they are slightly different. Consequently, different evolution of the T_g's of solid dispersions can be obtained from both experimental methods. The other explanation of the observed discrepancy is that both experimental techniques probe different kind of motions of molecules. One can remind that dielectric spectroscopy is sensitive to the rotation while DSC captures both rotation and translation motions of molecules. In view of these considerations it is obvious that k parameters obtained from the fitting data in Fig. 6a and b can be different.

It is also worth noting, that there are two independent approaches that enable approximation of k parameter in the Gordon Taylor equation. The first one is based on the free volume theory. Accordingly to this concept the constant k can be calculated by the Simha-Boyer rule (103):

$$k \approx \frac{T_g^{IMC} \rho^{IMC}}{T_g^{acMAL} \rho^{acMAL}} = \frac{314.5 * 1.377}{326.5 * 1.370} = \frac{433.07}{447.31} = 0.97 \tag{6}$$

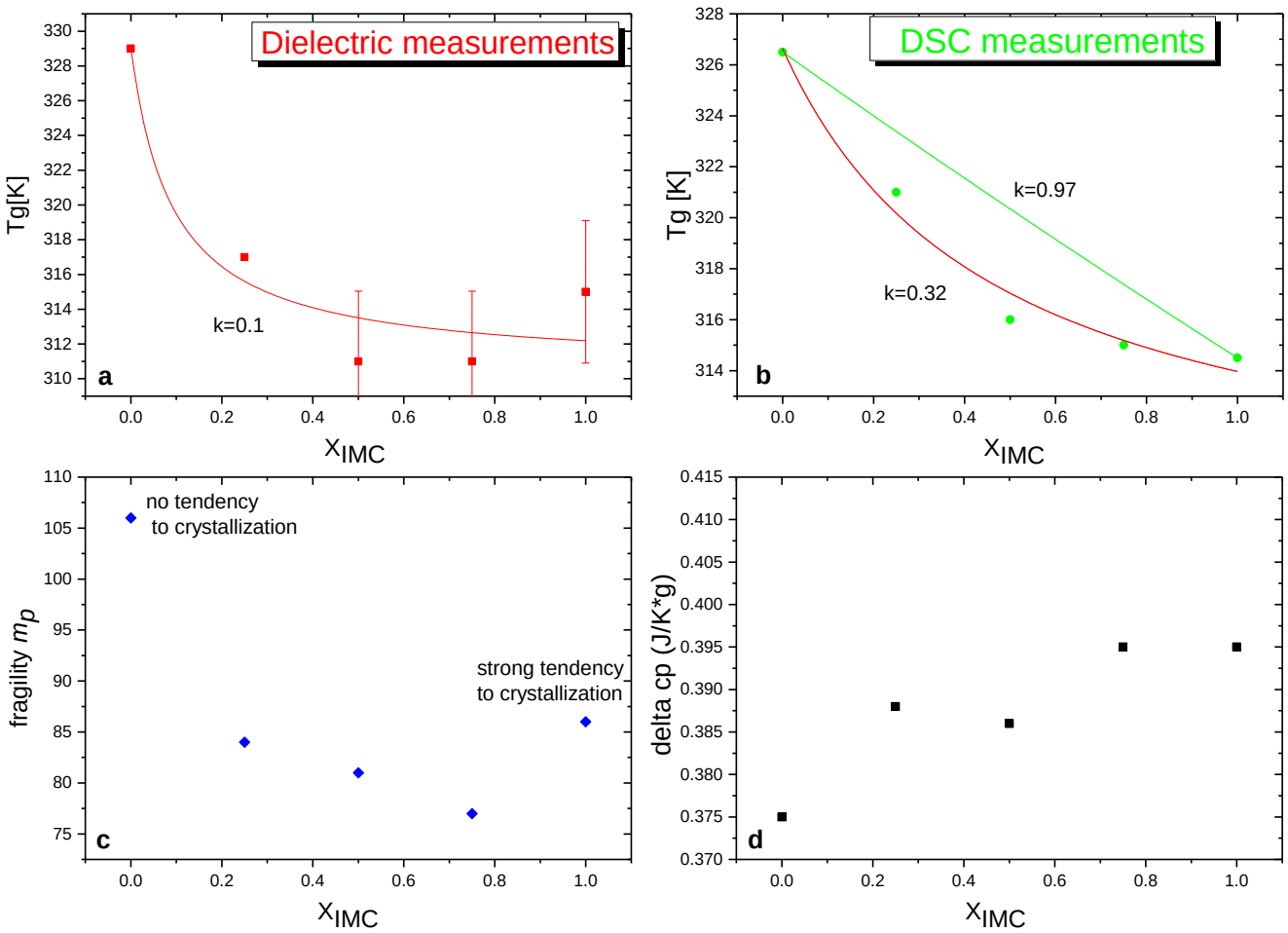

Fig. 6 Glass-transition temperatures T_g obtained from dielectric (**a**) and DSC (**b**) measurements vs weight fraction of indomethacin (X_{IMC}). Panels (**c**) and (**d**) present the dependence of the isobaric fragility estimated from Eq. 8 and heat capacity jump at T_g *versus* X_{IMC}, respectively. The *red lines* are the best fits to the data using Gordon – Taylor equation (Eq. 5).

where ρ^{IMC} and ρ^{acMAL} are densities of amorphous indomethacin and octaacetylmaltose.

Unfortunately, we were not able to measure ρ of amorphous components. Thus, densities of crystalline IMC and modified carbohydrate (http://www.chem-info.com) (96) were used. However, it should be noted that density of the amorphous compounds should be approximately 5% lower than the crystal ones (for example, as reported in literature, $\rho^{IMC\ amorphous}$ and $\rho^{IMC\ crystal}$ are equal 1.31 and 1.38 g/cm^3, respectively (40,96)). Therefore, results of calculations seems to be reliable.

The other approach to evaluate k is a Couchman-Karasz thermodynamical model (104). Accordingly to this concept k can be approximated by the following formula:

$$k \approx \frac{\Delta c_p^{acMAL}}{\Delta c_p^{IMC}} = \frac{0.375}{0.395} = 0.95 \qquad (7)$$

where $\Delta c_p{}^{acMAL}$ and $\Delta c_p{}^{IMC}$ are the amplitude of the c_p jump at T_g (or denote the change in heat capacity at T_g) determined for pure acMAL and pure indomethacin.

It is interesting to point out that despite of probing completely different properties of pure components both used herein models yielded almost the same k. Moreover, it should be noted that k approximated by the free volume and thermodynamical approaches is significantly different than the one obtained from the fitting data presented in Fig. 6 - panel b (k=0.32). Such pronounced discrepancy indicates that there must be strong interactions between IMC and octaacetylmaltose causing negative deviations from the predicted ideal behavior. To confirm this supposition, additional measurements by using Infrared Spectroscopy (IR) were carried out. Results of these investigations will be discussed in the further part of this paper.

In Fig. 6 (panel c) the dependence of the isobaric fragility (the steepness index) – m_p *versus* weight fraction of IMC is also presented. In light of the current discussion m_p seems to be very important single parameter that is used to characterize dynamics of given glass former. Isobaric fragility for all studied systems was calculated using the following formula (105):

$$m_p = \left.\frac{d\log_{10}\tau_\alpha}{d\left(T_g/T\right)}\right|_{T=T_g} \quad (8)$$

The estimated values are: m_p=86 (IMC), m_p=106 (acMAL), m_p=77 (IMC - acMAL 3 : 1), m_p=81 (IMC - acMAL 1 : 1) and m_p=84 (IMC - acMAL 1 : 3) - see also Table II. IMC and acMAL are the most fragile liquids from all investigated systems. This observation seems to be quite interesting. One could expect fragilities of solid dispersions to lie within the range 86–106, as estimated for pure components. Hence, this is another indication that there are probably strong interactions between IMC and modified carbohydrate affecting dynamics of solid dispersions above the glass transition temperature.

Additionally, in Fig. 6 (panel d) we have presented the dependence of Δc_p (heat capacity jump at T_g) vs X_{IMC}. As can be seen, the values of Δc_p calculated for both pure components and their mixtures in a 3 : 1, 1 : 1 and 1 : 3 weight ratios are very similar, they change to a limited extent (from 0.375 to 0.395 J/K*g)—see Table II.

In the next step, the solid dispersions of IMC and octaacetylmaltose were investigated by X-ray powder diffraction (XRD) technique to check recrystallization ability of IMC stored at room temperature. In Fig. 7 diffraction patterns measured for crystalline carbohydrate, indomethacin as well as two representative API - carbohydrate solid dispersions (3 : 1 and 1 : 3 weight ratios) after 1.5 year of storage at room temperature are shown. It can be seen that in the case of both mixtures there are no sharp Bragg peaks in diffractograms indicating crystallinity of the samples. Instead of that a broad amorphous halo consisted of three humps is observed. For the solid dispersion of IMC and acMAL (1 : 3 weight ratio) the maximum of the first part of amorphous halo up to 5 deg in 2Theta scale is located around 3.5 deg. One can add that it corresponds to the intermolecular distances (D) between molecules in the amorphous state, in the real space. Using the following formula $D=\lambda/2\cdot\sin\theta$ the average distance between molecules D=9.2 Å was obtained. It can be seen that for IMC-acMAL mixture (3 : 1 weight ratio) the first broadening peak is slightly shifted towards higher value of 2Theta, since the average distance between the molecules becomes smaller. Next two broadening peaks in the amorphous halos of both solid dispersions correspond to the intramolecular distances in the real space, and are also strongly correlated to the crystalline peaks.

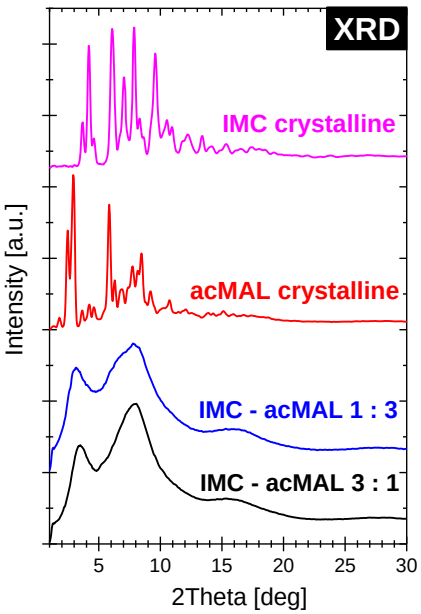

Fig. 7 Representative X-Ray powder diffraction patterns obtained for the crystalline IMC and acMAL as well as for the solid dispersions of IMC with acMAL in a 3 : 1 weight ratio (*black line*) and 1 : 3 weight ratio (*blue line*).

In addition, prolonged X-ray studies have also shown that IMC-acMAL binary mixtures are physically stable even after 1.5 year of storage at ambient conditions. In this context it should be noted that vitrified indomethacin recrystallizes when stored even 100 K below the glass transition temperature during such time.

Thus, one can ask the question what is the main factor that prevents recrystallization of indomethacin from the binary mixtures. Our studies with the use of dielectric spectroscopy showed that molecular dynamics of solid dispersions is not much different from the pure components to be responsible for the prolonged stability of IMC. Taking into account that preparation of the samples was the same in each case we supposed that probably strong intermolecular interactions between matrix and API might be the most important factor controlling physical stability of the solid dispersions. Especially that dielectric and calorimetric data provided some indications justifying such statement. To verify this thesis further measurements with the use of FTIR spectroscopy were carried out. It should be added that to get more insight into intramolecular interactions between octaacetylmaltose and indomethacin four additional IMC – acMAL binary mixtures (1 : 5, 5 : 1, 1 : 2 and 2 : 1 weight ratios) were prepared.

Experimental investigations supported by theoretical computations demonstrated that in the γ-form of crystalline IMC, molecules tend to form dimeric structures connected via strong hydrogen bonds (O-H-…-O) of interatomic distance about 1.66Å (18,97,106). To study intermolecular interactions between octaacetylmaltose and IMC we have selected several characteristic bands associated with the formation of IMC dimers. The infrared spectra of crystalline and amorphous indomethacin are presented in Fig. 8a. The characteristic bands related to the formation of dimers are detected at 1,223 cm^{-1}, 1,469 cm^{-1}, 1,709 cm^{-1} (supercooled liquid), 1,716 cm^{-1} (crystal) as well as in the 2,500–3,300 cm^{-1} range (97). The bands at 1,469 cm^{-1}, 1,709/1,716 cm^{-1} originate from the deformation vibration of βCOH group and stretching vibration of the νC=O unit in O=COH chain, respectively. The band located at 1,684 (supercooled liquid)/1,692 (crystal) cm^{-1} originates from the stretching vibration of benzoyl νC=O group. Additionally, the band at 1,735 cm^{-1}

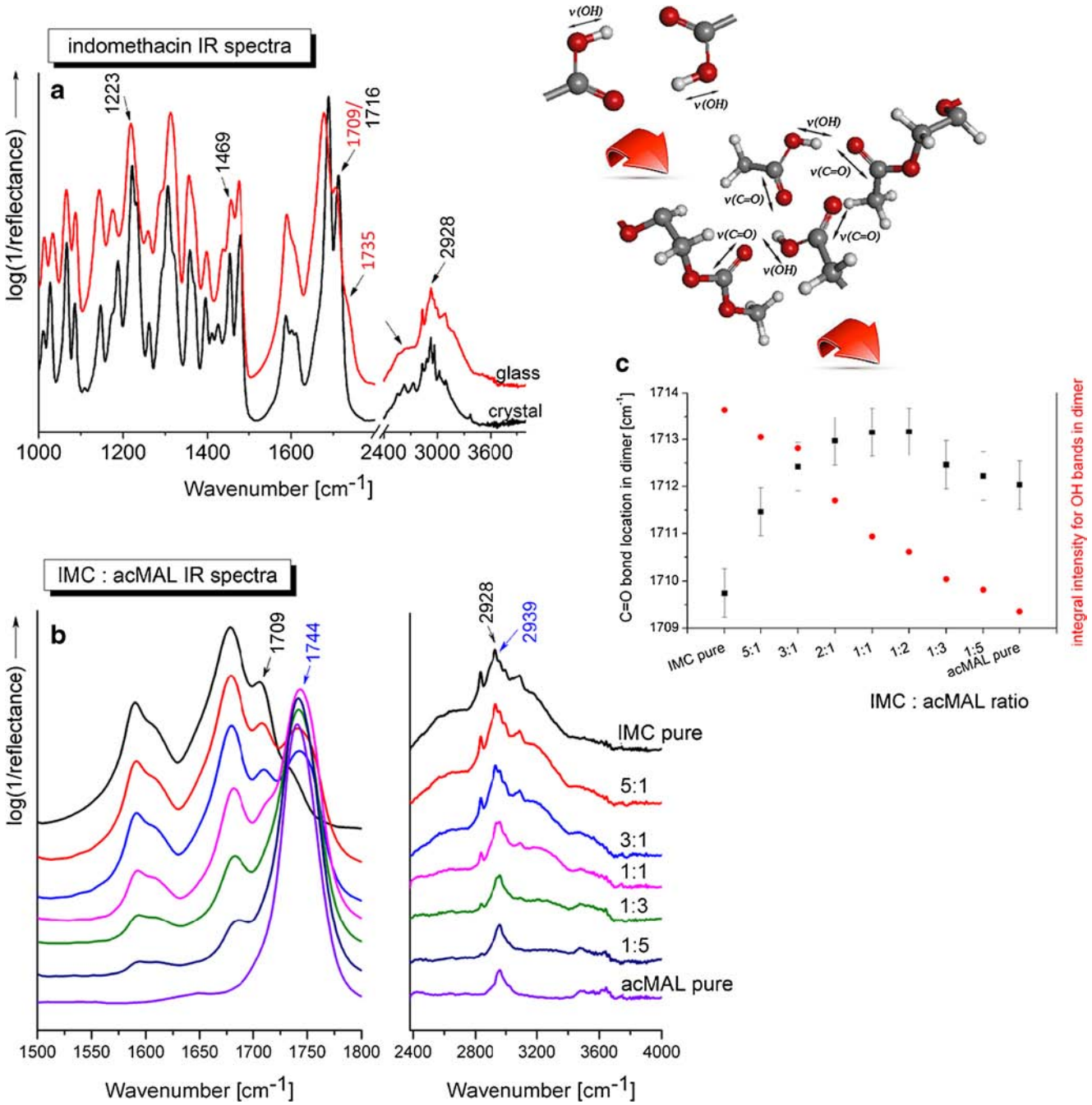

Fig. 8 FTIR spectra of: (**a**) crystalline and supercooled IMC, (**b**) IMC - acMAL binary mixtures with different weight ratios of both compounds, (**c**) integral intensity of the OH bands in 2,580–2,740 cm^{-1} region as well as change in position of the C = O band at 1,709 cm^{-1} *versus* acMAL content.

which Taylor *et al.* (18) assigned to the non-hydrogen bonded carbonyl stretch can be seen in the spectrum recorded for the supercooled liquid. The band located at 2,580–2,740 cm^{-1} was assigned to vibrations of the hydroxyl groups, and can be additionally connected to the formation of IMC dimers. It is worth to note that these bands are shifted towards lower frequencies due to formation of very strong hydrogen bonds in the dimeric structure (18,97,106). Strachan *et al.* (97) showed that bands at 2,928 (crystal) and 2,930 (supercooled liquid) cm^{-1} can also be assigned to the IMC dimers.

It is well known that octaacetylmaltose can act as a proton acceptor (through the O atom in the acetyl group), while indomethacin can be treated as a proton donor. Therefore, intermolecular interactions between acMAL and IMC should be well reflected in the acid carbonyl as well as in the hydroxyl stretching vibrations of both compounds (18). The infrared spectra of pure compounds and their binary mixtures of different weight ratios are presented in Fig. 8b. Strong influence of acMAL on the population of indomethacin dimers is clearly visible. The gradual increase of octaacetylmaltose

concentration leads to transformation of the double band at 1,735 cm^{-1} into a single peak at 1,744 cm^{-1}. Moreover, the shift of the vibration related to the acid carbonyl at 1,709 cm^{1} in IMC is observed. One can add that location of this band yields important information about the strength of H-bonds. The stronger they are the greater red shift of this band is observed. It should be noted that at the first glance this band moves only slightly in the FTIR spectra. However, careful fitting analysis indicated that the band at 1,709 cm^{-1} shifts to 1,713 cm^{-1} for IMC - acMAL binary mixture (1 : 2 weight ratio)—see Fig. 8c. The subsequent increase of acMAL concentration leads to slight movement of this band in the opposite direction. Simultaneously a continuous significant decrease of the integral intensity of the bands associated with the hydroxyl stretching vibrations (2,580–2,740 cm^{-1}) in dimeric structures is noted. One can mention that the integral intensity in the OH absorption bands was found to be more than 80% lower than that of the pure IMC in the solid dispersion prepared in the 1 : 1 weight ratio. Finally, it should be also noted that we have observed systematic significant shift of the band located at 2,928 cm^{-1} to 2,939 cm^{-1} (see Fig. 8b) in the absorption spectra measured for the binary mixtures. All these experimental findings clearly show that population of non- internally bonded indomethacin molecules grows up with increasing concentration of acMAL. Moreover, intermolecular interactions between IMC and modified carbohydrate become stronger with increasing concentration of the latter compound. Above a certain point corresponding roughly to the molar stoichiometric concentration intermolecular hydrogen bonded interactions between IMC and acMAL overcome IMC-IMC ones. As a consequence of that H-bonds between API and acetyl groups of octaacetylmaltose are formed at the expense of dimers. Although, these specific interactions are weaker than the ones observed in indomethacin dimeric structures. Similar results were reported by Taylor *et al.* for solid dispersions formed by IMC and PVP (18).

The intermolecular interactions between API and acMAL were also studied as a function of temperature. For that purpose temperature-dependent FTIR measurements on representative solid dispersion (1 : 1 weight ratio) were performed (see Fig. 9). The integral intensity analysis of bands associated with the vibrations of vC=O in a cyclic dimer (1,709 cm^{-1}) and vC=O in benzoyl (1,684 cm^{-1}) plotted as a function of temperature is given in Fig. 9. Both bands evolve in a very similar manner. The integral intensity analysis at room temperature shows a strong interaction between indomethacin and octaacetylmaltose. The IMC-acMAL solid dispersion is stable up to 313 K which corresponds to the calorimetric and dielectric glass transition temperature (T_g). Above T_g intermolecular interaction between IMC and modified carbohydrate becomes much weaker and IMC dimers tend to rebuild. In the range of temperature from 325 K up to 345 K dimers' population grows up. At temperatures higher than 350 K H-bonds between IMC dimers are getting weaker due to high thermal energy. Consequently, the population of IMC monomers increases, so they start to interact again with acMAL. However, these interactions are not as strong as at room temperature. A very similar pattern of behavior was observed for other binary mixtures of IMC with acMAL.

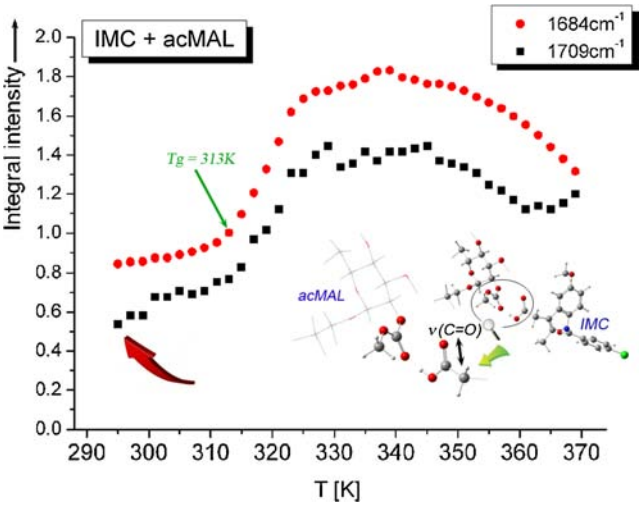

Fig. 9 Temperature-dependent integral intensity analysis for bands at 1,684 and 1,709 cm^{-1} for the representative binary system of IMC and acMAL (1: 1 weight ratio).

In the next step we have performed QSAR calculations to determine the impact of octaacetylmaltose on the indomethacin activity in the binary system. Molecular electrostatic potential maps of pure indomethacin (as a reference) and indomethacin-octaacetylmaltose system are shown in Fig. 10. Positively (blue) and negatively (red) charged groups indicate proton donors and acceptors, respectively. It can be seen that substantial negative charge for pure indomethacin is accumulated on the benzoyl C=O group as well as on dimers (i.e. on acid carbonyl and lone pairs of oxygen in hydroxyl groups). It is worth noting that due to formation of dimeric structures hydroxyl group can't act as a proton donor. The negative charge in pure octaacetylmaltose is accumulated mainly on C=O group of acetyl moiety, while the positive charge can be found on methyl groups. For IMC-acMAL system a significant change in electrostatic potential can be observed. In the case of solid dispersion there is no hydrogen bonds between two IMC molecules (see Fig. 10). Instead of that interactions with modified carbohydrate can be observed. The QSAR analysis has confirmed conclusions derived from FTIR measurements.

As a final point we have performed solubility studies of pure API and solid dispersion with acMAL. As demonstrated in Fig. 11, solubility of amorphous IMC increases with increasing content of modified carbohydrate in all studied herein media. What is more, in the case of IMC-acMAL mixture (1 : 5 weight ratio) solubility of IMC was 5-folds greater with

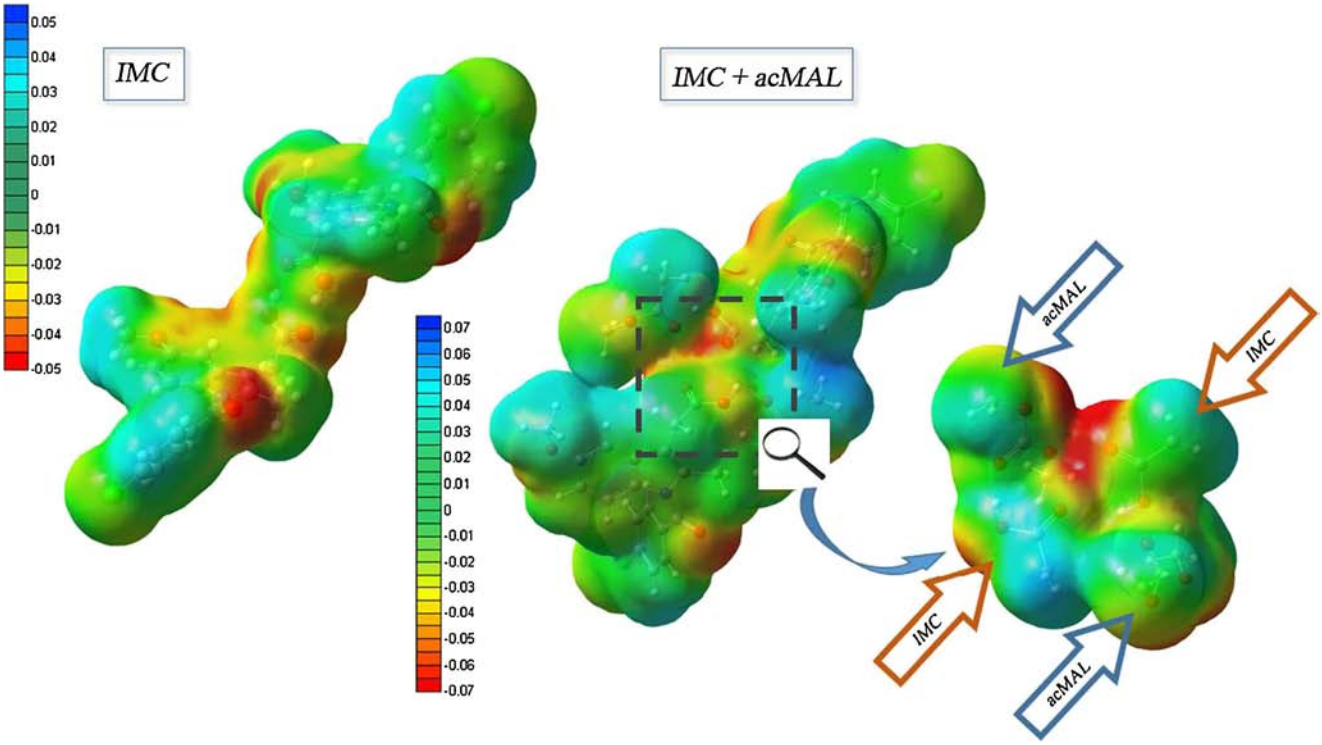

Fig. 10 The electrostatic surfaces potential for pure indomethacin (*left*) and indomethacin-octaacetylmaltose system (*right*) calculated by using DFT/B3LYP/6-31G(d,p) calculations [created in GaussView 5.0 based on Gaussian 09 calculations].

respect to the crystalline form and only slightly better than that of amorphous IMC. It is probably due to the strong intermolecular interactions between API and modified carbohydrate. Nevertheless, this is very balanced result that shows great potential of acMAL to prevent crystallization of labile APIs, as well as to improve their solubility.

CONCLUSIONS

In this paper we have investigated the impact of the low-molecular weight excipient, octaacetylmaltose (acMAL), on the physical stability of amorphous indomethacin (IMC). Several experimental techniques such as differential scanning calorimetry, dielectric and Raman spectroscopies were employed to characterize thoroughly physicochemical properties of investigated samples. We have found out that each sample is homogeneous in the whole range of studied temperatures. Amorphous solid dispersion of IMC with acMAL is physically stable for more than 1.5 year, so far. Based on FTIR studies one can conclude that intermolecular interactions between octaacetylmaltose and IMC are very strong and in fact more favorable than IMC - IMC ones. Therefore, hydrogen bonds between acetylated maltose and IMC are formed at the expense of indomethacin dimers. Analogical conclusion was also derived from QSAR calculations. Finally, solubility analysis revealed that acetyl derivative of maltose not only stabilizes the amorphous drug, but also enhances its solubility.

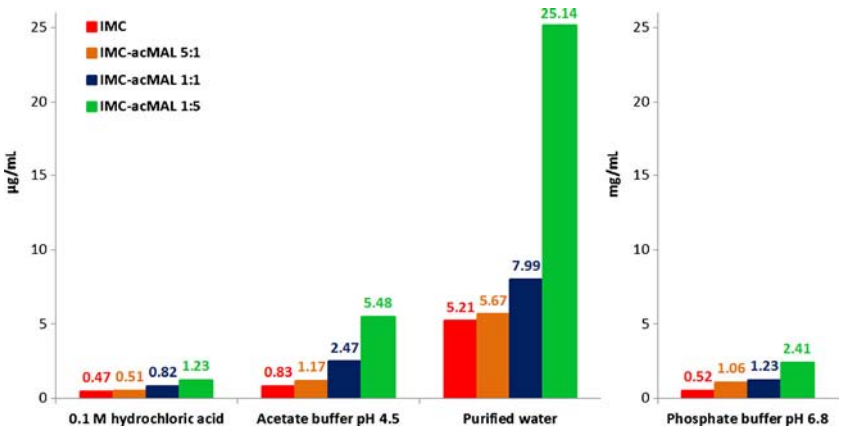

Fig. 11 Solubility of crystalline IMC and representative IMC – acMAL solid dispersions in different media.

ACKNOWLEDGMENTS AND DISCLOSURES

E.K., M.T., M.D. are thankful for the financial support from the National Center of Science based on decision DEC-2013/09/D/NZ7/04194. The authors are also thankful to Dr. M. Kopras from GlaxoSmithKline Pharmaceuticals S.A. (Poznan, Poland) for providing indomethacin. We would like to thank Dr M. Jarek from NanoBioMedical Centre (Poznan, Poland) for performing DSC measurements.

This research was supported in part by PL-Grid Infrastructure.

REFERENCES

1. Schuna AA. Update on treatment of rheumatoid arthritis. J Am Pharm Assoc. 1998;38:728–35.
2. Sweetman SC. Martindale: the complete drug reference. London: Pharmaceutical Press; 2005. p. 47.
3. Rodriguez LA, Varas C, Patrono C. Differential effects of aspirin and non-aspirin nonsteroidal antiinflammatory drugs in the primary prevention of myocardial infarction in postmenopausal women. Epidemiology. 2000;11:382–7.
4. Flynn BL, Theesen KA. Pharmacologic management of Alzheimer disease part III: nonsteroidal antiinflammatory drugs–emerging protective evidence? Ann Pharmacother. 1999;33:840–9.
5. Jones MK, Wang H, Peskar BM, Levin E, Itani RM, Sarfels IJ, *et al.* Inhibition of angiogenesis by nonsteroidal anti-inflammatory drugs: insight into mechanisms and implications for cancer growth and ulcer healing. Nat Med. 1999;5:1418–23.
6. Simmons DL, Botting RM, Hla T. Cyclooxygenase isozymes: the biology of prostaglandin synthesis and inhibition. Pharm Rev. 2004;56:387–437.
7. Weigert G, Berisha F, Resch H, Karl K, Schmetterer L, Garhofer G. Effect of unspecific inhibition of cyclooxygenase by indomethacin on retinal and choroidal blood flow. Invest Ophthalmol Vis Sci. 2008;49:1065–70.
8. Yamamoto T, Nozaki-Taguchi N. Analysis of the effects of cyclooxygenase (COX)-1 and COX-2 in spinal nociceptive transmission using indomethacin, a non-selective COX inhibitor, and NS-398, a COX-2 selective inhibitor. Brain Res. 1996;739:104–10.
9. Dressman J, Butler J, Hempenstall J, Reppas C. The BCS: where do we go from here. Pharm Technol. 2001;25:68–76.
10. Amidon GL, Lennernäs H, Shah VP, Crison JR. A theoretical basis for a biopharmaceutic drug classification: the correlation of in vitro drug product dissolution and in vivo bioavailability. Pharm Res. 1995;12:413–20.
11. Lobenberg R, Amidon GL. Modern bioavailability, bioequivalence and biopharmaceutics classification system; new scientific approaches to international regulatory standards. Eur J Pharm Biopharm. 2000;50:3–12.
12. Ford JL. The current status of solid dispersions. Pharm Acta Helv. 1986;61:69–88.
13. Hancock BC, Zografi G. Characteristics and significance of the amorphous state in pharmaceutical systems. J Pharm Sci. 1997;86:1–12.
14. Martin A. Physical pharmacy. 4th ed. Philadelphia: Lea and Febiger; 1993.
15. Kaminski K, Kaminska E, Adrjanowicz K, Grzybowska K, Wlodarczyk P, Paluch M, *et al.* Dielectric relaxation studies on Tramadol monohydrate and its hydrochloride salt. J Pharm Sci. 2010;99:94–106.
16. Adrjanowicz K, Kaminski K, Paluch M, Wlodarczyk P, Grzybowska K, Wojnarowska Z, *et al.* Dielectric relaxation studies and dissolution behavior of amorphous verapamil hydrochloride. J Pharm Sci. 2010;99:828–39.
17. Hancock BC, Parks M. What is the true solubility advantage for amorphous pharmaceuticals. Pharm Res. 2000;17:393–414.
18. Taylor LS, Zografi G. Spectroscopic characterization of interactions between PVP and indomethacin in amorphous molecular dispersions. Pharm Res. 1997;14:1691–8.
19. Adrjanowicz K, Zakowiecki D, Kaminski K, Hawelek L, Grzybowska K, Tarnacka M, *et al.* Molecular dynamics in supercooled liquid and glassy states of antibiotics: azithromycin, clarithromycin and roxithromycin studied by dielectric spectroscopy. Advantages given by the amorphous state. Mol Pharm. 2012;9:1748–63.
20. Serajuddin AT. Solid dispersion of poorly water-soluble drugs: early promises, subsequent problems, and recent breakthroughs. J Pharm Sci. 1999;88:1058–66.
21. Leuner C, Dressman J. Improving drug solubility for oraldelivery using solid dispersions. Eur J Pharm Biopharm. 2000;50:47–60.
22. Valizadeh H, Nokhodchi A, Qarakhani N, Zakeri-Milani P, Azarmi S, Hassanzadeh D, *et al.* Physicochemical characterization of solid dispersions of indomethacin with PEG 6000, Myrj 52, lactose, sorbitol, dextrin, and Eudragit E100. Drug Dev Ind Pharm. 2004;30:303–17.
23. Jung MS, Kim JS, Kim MS, Alhalaweh A, Cho W, Hwang SJ, *et al.* Bioavailability of indomethacin-saccharin cocrystals. J Pharm Pharmacol. 2010;62:1560–8.
24. Sato T, Okada A, Sdekiguchi K, Tsuda Y. Differences in physicopharmaceutical properties between crystalline and noncrystalline 9,3'diacetylmidecamycin. Chem Pharm Bull. 1981;29:2675–82.
25. Fukuoka E, Makita M, Yamamura S. Some physicochemical properties of glassy indomethacin. Chem Pharm Bull. 1986;34:4314–21.
26. Bhardwaj SP, Suryanarayanan R. Molecular mobility as an effective predictor of the physical stability of amorphous trehalose. Mol Pharm. 2012;9:3209–17.
27. Corrigan OI, Holohan EM, Sabra K. Amorphous forms of thiazide diuretics prepared by spray-drying. Int J Pharm. 1984;18:195–200.
28. Craig DQM, Royall PG, Kett VL, Hoptopn ML. The relevance of the amorphous state to pharmaceutical dosage forms: glassy drugs and freeze dried systems. Int J Pharm. 1999;179:179–207.
29. Adrjanowicz K, Kaminski K, Grzybowska K, Hawelek L, Paluch M, Gruszka I, *et al.* Effect of cryogrinding on chemical stability of the sparingly water-soluble drug furosemide. Pharm Res. 2011;28:3220–36.
30. Hedoux A, Guinet Y, Capet F, Paccou L, Decamps M. Evidence for a high-density amorphous form in indomethacin from Raman scattering investigations. Phys Rev B. 2008;77:094205.
31. Wojnarowska Z, Adrjanowicz K, Wlodarczyk P, Kaminska E, Kaminski K, Grzybowska K, *et al.* Broadband dielectric relaxation study at ambient and elevated pressure of molecular dynamics of pharmaceutical: indomethacin. J Phys Chem B. 2009;113:12536.
32. Dawsona KJ, Kearns KL, Lian Y, Steffenc W, Ediger MD. Physical vapor deposition as a route to hidden amorphous states. Proc Natl Acad Sci U S A. 2009;106:15165–70.
33. Kearns KL, Swallen SF, Ediger MD, Wu T, Yu L. Influence of substrate temperature on the stability of glasses prepared by vapor deposition. J Chem Phys. 2007;127:154702.
34. Kearns KL, Swallen SF, Ediger MD, Sun Y, Yu L. Calorimetric evidence for two distinct molecular packing arrangements in stable glasses of indomethacin. J Phys Chem B. 2009;113:1579–86.
35. Babu NJ, Nangia A. Solubility advantage of amorphous drugs and pharmaceutical cocrystals. Cryst Growth Des. 2011;11:2662–79.

36. Murdande SB, Pikal MJ, Shanker RM, Bogner RH. Solubility advantage of amorphous pharmaceuticals: II. Application of quantitative thermodynamic relationships for prediction of solubility enhancement in structurally diverse insoluble pharmaceuticals. Pharm Res. 2010;27:2704–14.
37. Karmwar P, Graeser K, Gordon KC, Strachan CJ, Rades T. Effect of different preparation methods on the dissolution behaviour of amorphous indomethacin. Eur J Pharm Biopharm. 2012;80:459–64.
38. Pikal MJ, Lukes AL, Lang JE, Gaines K. Quantitative crystallinity determinations for beta-lactam antibiotics by solution calorimetry: correlations with stability. J Pharm Sci. 1978;67:767.
39. Hancock BC, Carlson GT, Ladipo DD, Langdon BA, Mullarney MP. Comparison of the mechanical properties of the crystalline and amorphous forms of a drug substance. Int J Pharm. 2002;241:73–85.
40. Yoshioka M, Hancock BC, Zografi G. Crystallization of indomethacin from the amorphous state below and above its glass transition temperature. J Pharm Sci. 1994;83:1700–5.
41. Shamblin SL, Hancock BC, Pikal MJ. Coupling between chemical reactivity and structural relaxation in pharmaceutical glasses. Pharm Res. 2006;23:2254–68.
42. Wojnarowska Z, Grzybowska K, Adrjanowicz K, Kaminski K, Paluch M, Hawelek L, *et al.* Study of the amorphous glibenclamide drug: analysis of the molecular dynamics of quenched and cryomilled material. Mol Pharm. 2010;7:1692–707.
43. Hancock BC, Shamblin SL, Zografi G. Molecular mobility of amorphous pharmaceutical solids below their glass transition temperatures. Pharm Res. 1995;1:799–806.
44. Tian W, Lian Y. Origin of enhanced crystal growth kinetics near Tg probed with indomethacin polymorphs. J Phys Chem B. 2006;110:15694–9.
45. Hancock BC, Shamblin SL. Molecular mobility of amorphous pharmaceuticals determined using differential scanning calorimetry. Thermochim Acta. 2001;380:95.
46. Vyazovkin S, Dranca I. Effect of physical aging on nucleation of amorphous indomethacin. J Phys Chem B. 2007;111:7283–7.
47. Shamblin SL, Tang X, Chang L, Hancock BC, Pikal MJ. Characterization of the time scales of molecular motion in pharmaceutically important glasses. J Phys Chem B. 1999;103:4113.
48. Hancock BC, Dupuis Y, Thibert R. Determination of the viscosity of an amorphous drug using thermomechanical analysis (TMA). Pharm Res. 1999;16:672.
49. DeGusseme A, Carpentier L, Willart JF, Descamps M. Molecular mobility in supercooled trehalose. J Phys Chem B. 2003;107:10879–86.
50. He R, Craig DQM. An investigation into the thermal behaviour of an amorphous drug using low frequency dielectric spectroscopy and modulated. J Pharm Pharmacol. 2001;53:41.
51. Carpentier L, Decressain R, Desprez S, Descamps M. Dynamics of the amorphous and crystalline alpha-, gamma-phases of indomethacin. J Phys Chem B. 2006;110:457–64.
52. Bhugra C, Shmeis R, Krill SL, Pikal MJ. Different measures of molecular mobility: comparison between calorimetric and thermally stimulated current relaxation times below Tg and correlation with dielectric relaxation times above Tg. J Pharm Sci. 2008;97:4498–515.
53. Correia NT, Moura Ramos JJ, Descamps M, Collins G. Molecular mobility and fragility in indomethacin: a thermally stimulated depolarisation currents study. Pharm Res. 2001;18:1767–74.
54. Moura Ramos JJ, Correia NT, Taveira-Marques R, Collins G. The activation energy at Tg and the fragility index of indomethacin, predicted from the influence of the heating rate on the temperature positron and on the intensity of the thermally stimulated depolarisation current peak. Pharm Res. 2002;19:1879–84.
55. Savolainen M, Heinz A, Strachan C, Gordon KC, Yliruusi J, Rades T, *et al.* Screening for differences in the amorphous state of indomethacin using multivariate visualization. Eur J Pharm Sci. 2007;30:113–23.
56. Crowley KJ, Zografi G. Cryogenic grinding of indomethacin polymorphs and solvates: assessment of amorphous phase formation and amorphous phase physical stability. J Pharm Sci. 2002;91:492–507.
57. Planinsek O, Zadnik J, Kunaver M, Srcic S, Godec A. Structural evolution of indomethacin particles upon milling: time-resolved quantification and localization of disordered structure studied by IGC and DSC. J Pharm Sci. 2010;99:1968–81.
58. Greco K, Bogner R. Crystallization of amorphous indomethacin during dissolution: effect of processing and annealing. Mol Pharm. 2010;7:1406–18.
59. Karmwar P, Graeser K, Gordon KC, Strachan CJ, Rades T. Investigation of properties and recrystallisation behaviour of amorphous indomethacin samples prepared by different methods. Int J Pharm. 2011;417:94–100.
60. Bates S, Zografi G, Engers D, Morris K, Crowley K, Newman A. Analysis of amorphous and nanocrystalline solids from their x-ray diffraction patterns. Pharm Res. 2006;23:2333–49.
61. Dalal SS, Ediger MD. Molecular orientation in stable glasses of indomethacin. J Phys Chem Lett. 2012;3:1229–33.
62. Tetsumi I, Uekama K. Pharmaceutical applications of cyclodextrins. III. Toxicological issues and safety evaluation. J Pharm Sci. 1997;86:147–62.
63. Lofsson T, Masson M. Cyclodextrins in topical drug formulations: theory and practice. Int J Pharm. 2001;22:15–30.
64. Lakshman JP, Cao Y, Kowalski J, Serajuddin AT. Application of melt extrusion in the development of a physically and chemically stable high-energy amorphous solid dispersion of a poorly water-soluble drug. Mol Pharm. 2008;5:994–1002.
65. Kaushal AM, Gupta P, Bansal AK. Amorphous drug delivery systems: molecular aspects, design and performance. Crit Rev Ther Drug Carrier Syst. 2004;21:133–93.
66. Van den Mooter G, Wuyts M, Blaton N, Busson R, Grobet P, Augustijns P, *et al.* Physical stabilisation of amorphous ketoconazole in solid dispersions with polyvinylpyrrolidone K25. Eur J Pharm Sci. 2001;12:261–9.
67. Wang X, de Armas HN, Blaton N, Michoel A, Van den Mooter G. Phase characterization of indomethacin in binary solid dispersions with PVP VA64 or Myrj 52. Int J Pharm. 2007;345:95–100.
68. Khodaverdi E, Khalili N, Zangiabadi F, Homayouni A. Preparation, characterization and stability studies of glassy solid dispersions of indomethacin using PVP and isomalt as carriers. Iran J Basic Med Sci. 2012;15:820–32.
69. Backensfeld T, Müller BW, Wiese M, Seydel JK. Effect of cyclodextrin derivatives on indomethacin stability in aqueous solution. Pharm Res. 1990;7:484–90.
70. Bogdanova S, Bontcheva E, Avramova N. Phase characterization of indomethacin in adsorbates onto hydroxyethylcellulose. Drug Dev Ind Pharm. 2007;33:900–6.
71. Ghanem AH, El-Sabbagh H, Abdel-Alim H. Stability of indomethacin solubilized system. Pharmazie. 1979;34:406–7.
72. Shamblin SL. The characteristics of sucrose-polymer mixtures in the amorphous state. Ph. D. Dissertation, The University of Wisconsins Madison, 1997.
73. Grzybowska K, Kaminski K, Paluch M, Hawelek L. Patent application "The composite based on celecoxib and method of formulation", date of application: 19.04.2011 r., No. of application: P.394614.
74. Grzybowska K, Paluch M, Wlodarczyk P, Grzybowski A, Kaminski K, Hawelek L, *et al.* Enhancement of amorphous celecoxib stability by mixing it with octaacetylmaltose: the molecular dynamics study. Mol Pharm. 2012;9:894–904.
75. Kaminska E, Adrjanowicz K, Kaminski K, Wlodarczyk P, Hawelek L, Kolodziejczyk K, *et al.* A new way of stabilization of furosemide upon cryogenic grinding by using acylated saccharides matrices.

The role of hydrogen bonds in decomposition mechanism. Mol Pharm. 2013;10:1824–35.
76. Becke AD. Density-functional thermochemistry. III. The role of exact exchange. J Chem Phys. 1993;98:5648–52.
77. Parr RG, Yang W. Density-functional theory of the electronic structure of molecules. Annu Rev Phys Chem. 1995;46:701–28.
78. Lee C, Yang W, Parr RG. Development of the Colle-Salvetti correlation-energy formula into a functional of the electron density. Phys Rev B. 1988;37:785–9.
79. Hehre WJ, Radom L, Schleyer PR, Pople JA. Ab initio molecular orbital theory. New York: Wiley; 1986. p. 20–9. 65–88.
80. Parr RG, Yang W. Density functional theory of atoms and molecules. New York: Oxford University Press; 1989. p. 142–97.
81. Burke K, Perdew JP, Wang Y. In: Dobson JF, Vignale G, Das MP, editors. Electronic density functional theory: recent progress and new directions. New York: Plenum; 1998.
82. Frisch MJ, Trucks GW, Schlegel HB, Scuseria GE, Robb MA, Cheeseman JR, *et al.* Gaussian 03W, Revision B. 05, Gaussian Inc., Pittsburgh PA, 2003.
83. Mahieu A, Willart JF, Dudognon E, Danède F, Descamps M. A new protocol to determine the solubility of drugs into polymer matrixes. Mol Pharm. 2013;10:560–6.
84. Kaminski K, Wlodarczyk P, Havelek L, Adrjanowicz K, Wojnarowska Z, Paluch M, *et al.* Comparative dielectric studies on two hydrogen-bonded and van der Waals liquids. Phys Rev E. 2011;83:061506.
85. Blochowicz T, Rössler EA. Beta relaxation versus high frequency wing in the dielectric spectra of a binary molecular glass former. Phys Rev Lett. 2004;92:225701.
86. Roland CM, Ngai KL. Segmental relaxation and the correlation of time and temperature dependencies in poly (vinyl methyl ether)/polystyrene mixtures. Macromolecules. 1992;25:363–7. Dynamical heterogeneity in a miscible polymer blend. Macromolecules. 1991;24:2261–5.
87. Capaccioli S, Kessairi K, Prevosto D, Lucchesi M, Ngai KL. Genuine Johari–Goldstein β-relaxations in glass-forming binary mixtures. J Non-Cryst Solids. 2006;352:4643–8.
88. Capaccioli S, Prevosto D, Kessairi K, Lucchesi M, Rolla P. Relation between the dispersion of α-relaxation and the time scale of β-relaxation at the glass transition. J Non-Cryst Solids. 2007;353:3984–8.
89. Kessairi K, Capaccioli S, Prevosto D, Lucchesi M, Rolla PA. Relaxation dynamics in *tert*-butylpyridine/tristyrene mixture investigated by broadband dielectric spectroscopy. J Chem Phys. 2007;127:174502.
90. Kessairi K, Capaccioli S, Prevosto D, Sharifi S, Rolla PA. Effect of temperature and pressure on the structural (α-) and the true Johari–Goldstein (β-) relaxation in binary mixtures. J Non-Cryst Solids. 2007;353:4273–7.
91. Power G, Vij JK, Johari GP. Relaxations and nano-phase-separation in ultraviscous heptanol-alkyl halide mixture. J Chem Phys. 2007;126:034512.
92. Kremer F, Schönhals A (eds). Broadband dielectric spectroscopy. Springer-Verlag, 2003, ISBN 978-3-540-43407-8.
93. Williams G, Watts DC. Non-symmetrical dielectric relaxation behavior arising from a simple empirical decay function. Trans Faraday Soc. 1970;66:80–5.
94. Kohlrausch R. Nachtrag uber die elastiche Nachwirkung beim Cocon und Glasladen. Ann Phys Leipzig. 1847;72:353–405.
95. Alvarez F, Alegria A, Colmenero J. Relationship between the time-domain Kohlrausch-Williams-Watts and frequency-domain Havriliak-Negami relaxation functions. Phys Rev B. 1991;44:7306–12.
96. Vyazovkin S, Dranca I. Physical stability and relaxation of amorphous indomethacin. J Phys Chem B. 2007;111:7283–7.
97. Strachan CJ, Rades T, Gordon KC. A theoretical and spectroscopic study of γ-crystalline and amorphous indomethacin. J Pharm Pharmacol. 2007;59:261–9.
98. Havriliak S, Negami S. A complex plane analysis of α- dispersions in some polymer systems. J Polym Sci C. 1966;14:99–117.
99. Vogel H. Das Temperaturabhangigkeitgesetz der Viskosität von Flüssigkeiten. J Phys Z. 1921;22:645–6.
100. Fulcher GS. Analysis of recent measurements of the viscosity of glasses. J Am Ceram Soc. 1925;8:339–55.
101. Tammann G, Hesse W. Die Abhängigkeit der Viscosität von der Temperatur bie unterkühlten Flüssigkeiten. Z Anorg Allg Chem. 1926;156:245–57.
102. Gordon M, Taylor JS. Ideal copolymers and the second-order transitions of synthetic rubbers. I. Non-crystalline copolymers. J Appl Chem. 1952;2:493–500.
103. Simha R, Boyer RF. On a general relation involving the glass temperature and coefficients of expansion of polymers. J Chem Phys. 1962;37:1003–7.
104. Couchman PR, Karasz FE. A classical thermodynamic discussion on the effect of composition on glass-transition temperatures. Macromolecules. 1978;11:117–9.
105. Angell CA. Relaxation in liquids, polymers and plastic crystals — strong/fragile patterns and problems. J Non-Cryst Solids. 1991;131–133:13–31.
106. Kirstenmacher TJ, Marsh RE. Crystal and molecular structure of an antiinflammatory agent, indomethacin, 1-(p-chlorobenzoyl)-5-methoxy-2-methylindole-3-acetic acid. J Am Chem Soc. 1972;94:1340–5.